Exploring the Effects of Glasses on mmWave: Attenuation, Thermal Impact, and Implications for 5G and Beyond Mobile Technologies

Md Jannatul Rakib Joy, Negin Foroughimehr, Ali Yavari
6G Research and Innovation Laboratory
School of Science, Computing and Engineering Technologies
Swinburne University of Technology
Melbourne, Australia
103799644@student.swin.edu.au, nforoughimehr@swin.edu.au, mail@aliyavari.com

***Abstract*—The growing demand for higher bandwidth has pushed mobile carrier frequencies into the millimeter-wave (mmWave) spectrum such as high-band 26 GHz, to meet the requirements of 5G networks and advanced communication technologies. While mmWave frequencies provide the necessary bandwidth for high-speed data transmission, they pose significant challenges, especially in urban environments where signals interact with common building materials like glass. This study focuses on the effects of 26 GHz mmWave propagation through various glass types commonly found in modern urban architecture. Our experiment measured electric field (E-field) strength loss, attenuation, and temperature variations as the waves passed through different glass samples. Results show that highly reflective and coated glass types, such as Low-E and silver reflective glass, caused significant E-field strength reduction reaching up to 93% . The experiment also revealed a noticeable temperature increase in some glass samples, further influencing signal degradation. These findings underline the importance of consideration of the glass materials as they can cause signal loss, impacting reliability of the 5G and beyond connectivity in urban environments.**

***Index Terms*—5G, millimeter-wave, 26 GHz, urban infrastructure, signal propagation, dielectric materials.**

I. Introduction

In the race to build faster, more reliable fifth-generation (5G) networks, the ability of 26 GHz signals to navigate dense urban environments is both promising and challenging. The evolution of wireless communication from fourth-generation (4G) to 5G represents a shift in how data is transmitted, processed, and utilized across various industries. Unlike its previous generation, 5G technology promises not only faster data speeds but also lower latency, increased capacity, and support for a much larger number of connected devices. These advancements make 5G the foundation for enabling emerging technologies such as autonomous vehicles, smart cities, augmented reality (AR), and the Internet of Things (IoT) [1]–[3]. To achieve these benefits, 5G relies on higher-frequency bands, specifically millimeter waves (mmWave), which offer the bandwidth necessary for handling massive data transfers in real time [4], [5].

One of the critical frequency bands for 5G deployment is 26 GHz, part of the lower mmWave spectrum. This frequency is crucial because it creates a balance between offering ultra-high data transfer speeds and maintaining a usable transmission range. Unlike traditional 4G frequencies that operate below 6 GHz, millimeter waves in the 24-52 GHz range offer significantly more bandwidth, allowing for high bandwidth applications that were previously unfeasible. However, the shift to mmWave frequencies, including 26 GHz, introduces new challenges, particularly in dense urban environments, where signal penetration and stability are critical.

While mmWave frequencies like 26 GHz offer tremendous potential, they also face significant challenges, primarily due to signal attenuation and interference. mmWaves have much shorter ranges than traditional sub-6 GHz frequencies, making them more vulnerable to environmental interference from materials such as buildings, glass, concrete, vegetation, and even atmospheric conditions [6], [7]. The higher the frequency, the more susceptible the signal is to physical obstructions. This makes the propagation of 26 GHz signals particularly difficult in urban areas, where physical objects constantly obstruct line-of-sight transmission.

Urban environments are filled with reflective and absorptive materials, including metal, concrete, and glass, which cause signal weakening, reflection, and scattering. As 5G signals attempt to navigate through densely packed city infrastructure, they encounter significant signal loss, reducing the effective communication range and requiring more frequent placement of 5G base stations. This presents a critical challenge for network designers tasked with optimizing 5G coverage in cities. Understanding how these signals interact with different building materials is crucial for improving network design, performance optimization and reliability.

The 26 GHz frequency band is crucial for 5G as it balances high data speeds and moderate range. However, it also faces significant challenges, such as signal attenuation and obstruction in urban environments. While ideal for transmitting large amounts of data in compact areas, 26 GHz signals are more susceptible to interference from materials like buildings, glass,

and metal, which can reflect or weaken the signal. Studies have also shown that rain attenuation at these frequencies is considerable, especially during heavy rainfall periods, further compromising signal penetration and transmission quality. This highlights the importance of studying how these signals behave in real-world environments to optimize network designs that ensure reliable 5G performance in urban settings [8].

This paper investigates the propagation characteristics of 26 GHz mmWave signals in urban environments, focusing on how different types of glass, commonly used in windows and facades, affect signal strength and temperature. By analyzing the attenuation and thermal effects of 26 GHz signals as they pass through various glass types, we aim to identify which glass causes the most signal loss and how much the temperature increases during transmission.

The remainder of this paper is structured as follows: Section II provides a review of existing literature on mmWave propagation in urban environments. Section III outlines the methodology, materials, and system architecture used in our experiments, including the setup for testing signal attenuation and temperature changes. Section IV presents and analyzes the results, focusing on key findings related to signal attenuation through different types of glass. Finally, Section V offers a summary of the findings and recommendations for future research to enhance the implementation of 5G in urban environments.

II. Related Work

The usage of 5G technology is expected to revolutionize connectivity due to significant improvements in data transfer speeds, bandwidth, and low latency, which are essential for advanced applications such as smart cities, autonomous vehicles, and augmented reality [9]. An essential aspect in enabling these developments is the use of mmWave frequencies, particularly in the 26 GHz region, which provides the high data throughput required for these innovations [10]. However, one of the key obstacles to the widespread deployment of 5G in densely populated urban areas is the interaction of mmWave signals with common building materials, particularly glass. Due to its absorptive and reflective properties, glass plays a critical role in determining the performance of 5G networks, making it a significant focus of research in optimizing signal propagation in urban environments [11], [12].

In urban environments, mmWave signal propagation faces significant challenges due to the presence of materials like glass, concrete, and metal, which either reflect or absorb the signals. Glass, in particular, poses difficulties for mmWave transmission because its dielectric properties cause reflection, absorption, and scattering of signals. Certain glass types, such as Low-E glass, can reflect up to 80% of incoming signals, severely affecting indoor coverage and overall network stability [13], [14]. Furthermore, when glass absorbs mmWave signals, it converts the electromagnetic energy into heat, which alters the glass's physical properties and impacts how the wave propagates [15]. These effects—reflection, absorption, and heat conversion—not only weaken signal strength but also contribute to complex interference patterns, making it challenging to maintain strong and reliable 5G network performance in densely populated urban areas [16].

Glass coatings, such as ultraviolet (UV) and solar control films, further complicate mmWave signal transmission by increasing both reflection and absorption. These coatings, designed for energy efficiency, can significantly disrupt 5G signals. The low E glass can lead to up to 20dB more signal attenuation compared to standard glass, underscoring the additional challenges posed by modern building materials [17]. In urban environments with tall buildings and large glass facades, these effects become even more pronounced, making it difficult to maintain consistent reliable 5G connectivity and requiring specific optimization strategies [18].

Beyond the direct signal loss caused by reflection and absorption, the interaction of mmWave signals with glass can also introduce thermal effects. When glass absorbs millimeter-wave frequencies, it converts the energy into heat, which affects its ability to transmit signals and further increases attenuation [19]. The challenges associated with mmWave propagation in urban environments are not merely theoretical but have been observed in practical implementations. Case studies from cities like Prato and L'Aquila provide critical insights into how materials and urban environments affect 5G performance, emphasizing the need for adaptive technologies like beam-forming and network slicing to maintain reliable signal quality in complex urban environments [20].

Given the substantial impact of glass on mmWave signal propagation, it is evident that specialized technological solutions are needed to optimize 5G performance in urban environments. Beamforming and beam-steering technologies, which dynamically adjust the direction of signals to avoid reflective obstructions, have shown significance in overcoming these challenges [21]. Advanced techniques like machine learning-driven adaptive beamforming enable real-time adjustments based on environmental feedback, improving signal quality by navigating around reflective surfaces like glass façades [22], [23]. Furthermore, advances in glass materials also hold great potential for reducing signal degradation. The development of new coatings that minimize reflection while maintaining energy efficiency could greatly enhance 5G performance in urban settings. Innovative approaches such as nanomaterial coatings, which can reduce signal reflection without compromising thermal insulation, offer a balanced solution to the challenges.

The integration of 5G technology into urban environments will require innovative solutions to overcome the significant challenges posed by the interaction between mmWave signals and modern glass materials. As highlighted by real-world studies in cities like Prato and L'Aquila, signal loss due to reflective and absorptive glass coatings is a critical issue that must be addressed.

III. Method and Material

Our experiment focused on analyzing the attenuation of 26 GHz mmWave as they passed through various glass types commonly used in windows, doors, and building structures in urban area. The experimental setup used for analyzing 26 GHz mmWave propagation through glass was designed by adapting the existing mmWave exposure system that operates between 26–40 GHz frequencies, as described by Foroughimehr et al. [24], [25]. This system was specifically adapted to evaluate how 26 GHz waves interact with different types of glass.

To ensure the accuracy of our results and minimize any system malfunctions or discrepancies, each experiment was conducted for at least 1 minute, and each test was repeated at least twice for verification. The entire experiment was conducted in an anechoic chamber, which helped eliminate unwanted reflections and interference from external signals, such as those from phones or other devices, ensuring accurate and uncontaminated measurements during the process. The core system components include a spot-focusing lens horn antenna, a signal generator, a RadMan2 - Personal radiation monitor, an infrared (IR) thermal camera, and power meters.

The core of our setup (shown in Figure 1) was a horn antenna that focused the mmWave radiation into a precise 1 cm focal point. This beam was directed at the glass sample, ensuring minimal wave dispersion. The signal was generated by an HP 8673B Synthesized Signal Generator operating at 26 GHz and amplified using the MI-WAVE 955 Series Power Amplifier to provide adequate power for signal propagation through the glass. The antenna's focal point was positioned exactly 133 mm away from the glass sample for optimal wave interaction.

The RadMan2 Personal Radiation Monitor was used to measure the E-field strength of the mmWave after it passed through the glass sample. This device was connected to a laptop via USB (as shown in Figure 1) for real-time data collection and monitoring. During the test, the RadMan2 monitor recorded the remaining percentage of the electric field after the wave passed through the glass, which was later converted into volts per meter (V/m) for calculating signal attenuation.

The frequency range of the RadMan2 is from 1 MHz to 60 GHz, making it ideal for monitoring the 26 GHz mmWave signals used in our study. The monitor provided percentage values that represented the level of exposure relative to the International Commission on non-ionizing Radiation Protection (ICNIRP) safety limit for occupational exposure (137 V/m).

To track thermal changes on the surface of the glass, an infrared (IR) thermal camera was used during the experiment. This camera monitored the temperature of the glass during the exposure to mmWaves, allowing us to determine how much wave energy was being absorbed as heat. Any significant increase in surface temperature would indicate energy absorption, which could affect signal transmission and contribute to attenuation.

The testbed is where we made slight modifications to accommodate the specific needs of our glass E-field measurements and attenuation experiments. The testbed, illustrated in Figure 1, securely holds the glass samples for precise and repeatable measurements.

Fig. 1. Testbed during test which is connected with a laptop to collect the result from the RadMan2 receiver.

The setup includes a custom-designed glass holder with a precision-aligned hole to ensure that the mmWave beam from the spot-focusing lens horn antenna passes directly through the glass. This precise alignment was essential to ensure consistent wave interaction across all samples, minimizing diffraction and ensuring that the E-field strength & attenuation results were comparable across different glass types.

A. Material

For this experiment, we used 23 unique glass samples to analyze the attenuation of 26 GHz mmWave. These glass samples were selected because they are commonly used in windows, doors, and building structures in urban environments. The experiment was designed to explore how different chemical compositions, colors, and thicknesses of glass influence their interaction with 26 GHz mmWave. In total, 43 experiments were conducted using various combinations of glass types and temperatures to account for different environmental conditions.

The 23 unique types of glass and their corresponding combinations are outlined in Table I.Here, we used 23 different types of glass, all of which had a width of 0.5 cm $\pm$ 1 mm. The temperature during the experiment was approximately 18°C unless otherwise specified.

B. Data Collection

For our data collection, we primarily relied on the RadMan2 Personal Radiation Monitor to measure the signal strength of the 26 GHz mmWave after it passed through each glass sample. The data collection process was facilitated by the RadMan 2-TS software, which allowed for real-time monitoring of the exposure levels.

Each test was conducted for 1 minute and repeated twice to ensure the accuracy and consistency of the results, eliminating the possibility of system malfunctions or discrepancies. The

TABLE I
TYPES OF GLASS USED IN THE EXPERIMENTS, ALONG WITH THE VARIOUS COMBINATIONS AND TEMPERATURE SETTINGS.

Glass ID	Glass Type	Glass ID	Glass Type
1	Clear float	24	Glass 19 and 6 combined
2	Navy blue reflective	25	Glass 19, 6 and 11 combined
3	Silver mirror	26	Glass 6 and 11 combined
4	Clear frosted	27	Glass 1 and 20 combined
5	Washing blue clear low-E glass	28	Glass 1 and 5 combined
6	Golden reflective	29	Glass 1 and 19 combined
7	Non-reflective Red 34	30	Glass 12, cold (8°C)
8	Black tinted	31	Glass 12, hot (43°C)
9	Coffee colored tinted	32	Glass 4, cold (4°C)
10	Ribbed obscured	33	Glass 4, hot (36°C)
11	Silver reflective	34	Glass 20, cold (6.1°C)
12	Black float	35	Glass 20, hot (38°C)
13	Crystal mirror blue	36	Glass 19, cold (6°C)
14	Coffee colored float	37	Glass 19, hot (39°C)
15	Obscured glass (dotted design)	38	Glass 11, cold (5 °C)
16	Washing blue reflective	39	Glass 11, hot (26°C)
17	European bronze tinted mirror	40	Glass 22, cold (7°C)
18	Clear frosted designed	41	Glass 22, hot (38°C)
19	Green reflective	42	Glass 1, cold (5°C)
20	Dark blackish blue float	43	Glass 1, hot (30°C)
21	Textured obscured		
22	Everglade fluted		
23	Light blue tinted		

percentage values recorded by the RadMan2 device were calculated relative to the ICNIRP safety limit for occupational exposure, and these values were then used in the calculation of signal attenuation.

C. E-field Strength Calculation

Power density (S), defined as the power per unit area perpendicular to the direction of propagation, is related to E-field and magnetic (H) fields by the Equation 1.

$$S = E \cdot H = \frac{E^2}{377} \tag{1}$$

According to ICNIRP guidelines, the E-field limits are:

$$E = \sqrt{377 \times S} \tag{2}$$

For occupational limits: $E = \sqrt{377 \times 50} = 137\,\text{V/m}$
For public limits: $E = \sqrt{377 \times 10} = 61.4\,\text{V/m}$

The E-field values were derived by converting the percentage readings from the RadMan2 device into volts per meter (V/m), using the ICNIRP exposure limit. The formula applied for this conversion was as follows:

$$E = \text{Percentage Value} \times (limit)\,\text{V/m} \tag{3}$$

This formula was applied across all glass samples to calculate both the initial E-field (E_initial) before the wave passed through the glass and the final E-field (E_final) after the wave had passed through. These values were used in the attenuation calculation.

We also collected temperature changes during the test using an IR Thermal camera. The E-field Strength loss, temperature values for all 43 glass combinations were calculated and shown in the Figure 2 and 3.

IV. RESULTS AND DISCUSSION

Our experimental results are visually represented in Figure 2, providing a comparison of E-field loss across all 23 unique glass types and a total of 43 total glass combinations.Temperature changes for the 23 unique glass samples are illustrated in Figure 3.

From the result, we observed that the E_initial values were consistent across all glass types. This consistency is critical for ensuring reliable baseline measurements, indicating that the wave generation and experimental setup were stable throughout the tests. However, the final E-field (E-final) values varied significantly based on the glass type.

For an unique glass type, the Silver reflective glass (Glass ID 11) had the highest electric field (E-field) loss. This significant reduction highlights the substantial impact of reflective coatings on signal strength at 26 GHz mmWave frequencies.

Conversely, glass types such as Non-Reflective Red 34 (Glass ID 7) and Everglade Fluted (Glass ID 22) demonstrated higher E-final values. This suggests that these glasses contain fewer reflective or absorptive materials, resulting in lower signal attenuation. The reduced interaction between the 26 GHz millimeter waves and these glass types indicates a minimal impact on signal strength, allowing the waves to pass through with less disruption.

The results indicate that the electric field loss varied considerably across both single and combination glass types, as shown in the Figure 3. The highest percentage of electric field loss was observed for Silver reflective glass (Glass ID 11), with a loss around 93%, making it highly unsuitable for mmWave transmission due to its high reflective properties. Similarly, the Green + golden + silver reflective glass combination (Glass ID 25) exhibited an extremely high electric field loss, exceeding 98%. This can be attributed to the multiple reflective coatings that severely disrupt wave propagation. These coatings increase reflection and absorption, leading to substantial power loss and making such glass types inefficient for mmWave transmission in 5G and beyond networks.

On the other hand, lower electric field losses were observed for glass types such as Non-Reflective Red 34 (Glass ID 7) and Ribbed Obscured glass (Glass ID 10), which exhibited losses of approximately 30% to 40%, respectively. The lower E-field loss for these glass types indicates minimal disruption to the 26 GHz mmWave propagation. This suggests that the less reflective or absorptive properties of these glasses allow the waves to pass through with minimal interference, making them more suitable for environments requiring efficient signal transmission, particularly in 5G networks.

Temperature changes, as measured by the IR thermal camera, provided important insights into the thermal absorption properties of the glass samples. For most samples, there was minimal temperature variation (less than 0.4°C), indicating that the absorption of mmWave energy did not lead to significant heat accumulation. However, certain glass types such

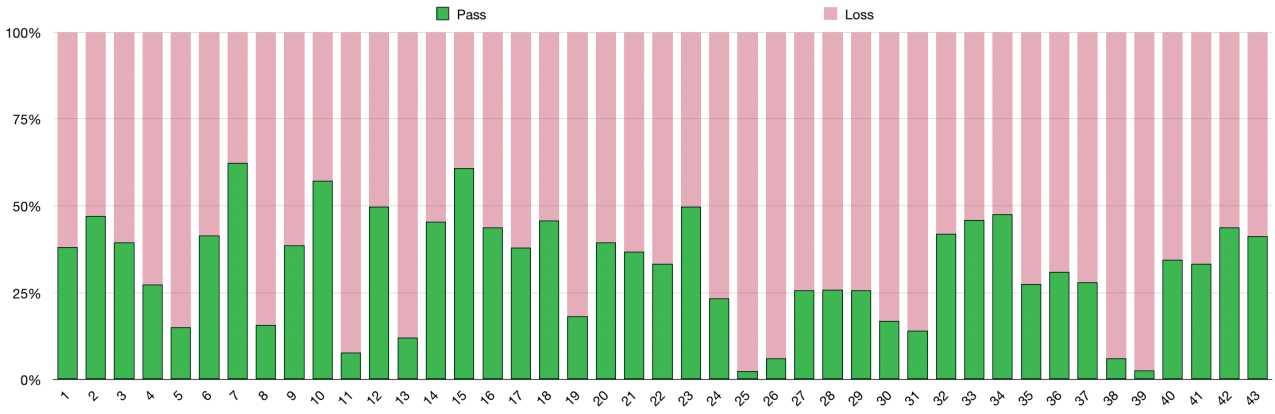

Fig. 2. Comparison of the e-field loss.

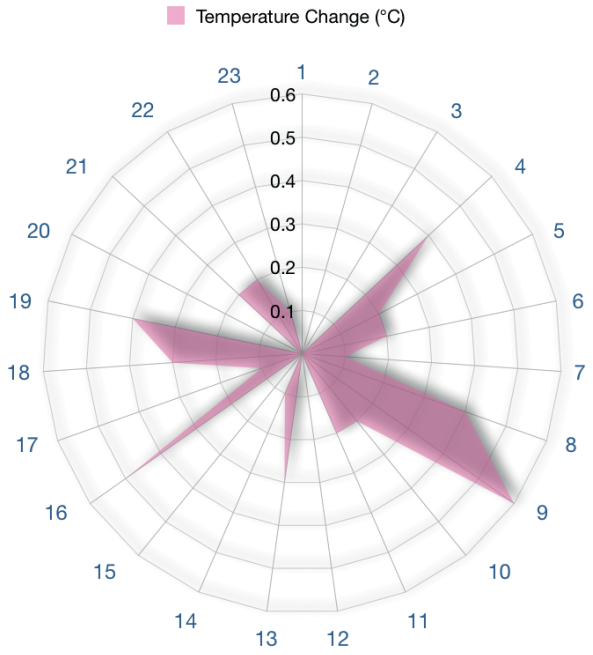

Fig. 3. Comparison of the temperature changes.

as crystal mirror blue glass, and Silver & blue reflective glass, which exhibited the highest electric field strength loss and signal attenuation, showed more considerable temperature increases, particularly under hotter conditions.

This correlation between increased temperature and higher attenuation suggests that glass types with more reflective or absorptive coatings not only disrupt signal propagation but also accumulate more heat when exposed to mmWave frequencies. For example, silver reflective glass (hot 26°C) demonstrated E-field strength loss of 98%, compared to 93% under room temperature (18°C) conditions. This further highlights the significant impact thermal effects have on mmWave signal transmission for specific glass types, particularly in environments with fluctuating temperature conditions.

The results from this study show that glass type, reflective coatings, and temperature conditions have a significant impact on mmWave signal attenuation. Reflective glasses, such as green, blue, or silver reflective glass, exhibited the highest attenuation, while non-reflective glass types like non-reflective float or tinted glass showed lower signal loss, making them better suited for 5G applications. These findings highlight the need of consideration of building materials in desiging future 5G networks.

V. Conclusion

This study highlights the critical impact that glass types, coatings, and temperature conditions have on the propagation of 26 GHz mmWave signals in urban environments. Through detailed analysis of various glass samples, we observed that highly reflective and coated glass, such as Low-E and silver reflective glass, caused significant signal attenuation and E-field strength loss. E-Field strength loss reached as high as 93% underscoring the challenges these materials pose for the reliable deployment of 5G networks. Furthermore, the interaction between mmWave signals and glass resulted in noticeable temperature increases, which further exacerbated signal degradation.

Our findings emphasize the importance of selecting glass materials with optimized dielectric properties to minimize signal loss and maintain reliable connectivity in densely populated urban areas. As 5G networks become integral to smart cities and high-data-rate applications, it is imperative that building materials, especially glass, are designed to support mmWave transmission.

References

[1] L. Cai, J. Wu, L. Lamberson, E. Streltsova, C. Daly, A. Zakharian, and N. F. Borrelli, "Glass for 5G applications," *Appl. Phys. Lett.*, vol. 119, no. 8, p. 082901, Aug. 2021.

[2] A. Yavari, "Internet of things data contextualisation for scalable information processing, security, and privacy," Ph.D. dissertation, RMIT University, 2019.

[3] A. Yavari, H. Korala, D. Georgakopoulos, J. Kua, and H. Bagha, "Sazgar iot: A device-centric iot framework and approximation technique for efficient and scalable iot data processing," *Sensors*, vol. 23, no. 11, p. 5211, 2023.

[4] H. Korala, D. Georgakopoulos, P. P. Jayaraman, and A. Yavari, "A time-sensitive iot data analysis framework," 2021.

[5] H. Korala, P. P. Jayaraman, A. Yavari, and D. Georgakopoulos, "Apollo: A platform for experimental analysis of time sensitive multimedia iot applications," in *Proceedings of the 18th International Conference on Advances in Mobile Computing & Multimedia*, 2020, pp. 104–113.

[6] N. Hosseini, M. Khatun, C. Guo, K. Du, O. Ozdemir, D. W. Matolak, I. Guvenc, and H. Mehrpouyan, "Attenuation of several common building materials: Millimeter-wave frequency bands 28, 73, and 91 ghz," *IEEE Antennas and Propagation Magazine*, vol. 63, no. 6, pp. 40–50, 2021.

[7] O. Putriani, S. Priyanto, I. Muthohar, and M. R. F. Amrozi, "Millimetre wave and sub-6 5g readiness of mobile network big data for public transport planning," *Sustainability*, vol. 15, no. 1, 2023.

[8] K. Ulaganathen, A. Tharek, R. M. Islam, and K. Abdullah, "Case study of rain attenuation at 26 ghz in tropical region (malaysia) for terrestrial link," in *2015 IEEE 12th Malaysia International Conference on Communications (MICC)*, 2015, pp. 252–257.

[9] T. S. Rappaport, S. Sun, R. Mayzus, H. Zhao, Y. Azar, K. Wang, G. N. Wong, J. K. Schulz, M. Samimi, and F. Gutierrez, "Millimeter wave mobile communications for 5g cellular: It will work!" *IEEE Access*, vol. 1, pp. 335–349, 2013.

[10] T. Bai and R. W. Heath, "Coverage and rate analysis for millimeter-wave cellular networks," *IEEE Transactions on Wireless Communications*, vol. 14, no. 2, pp. 1100–1114, 2015.

[11] T. Chaloun, S. Brandl, N. Ambrosius, K. Kröhnert, H. Maune, and C. Waldschmidt, "Rf glass technology is going mainstream: Review and future applications," *IEEE Journal of Microwaves*, vol. 3, no. 2, pp. 783–799, 2023.

[12] K. S. Muttair, O. A. Sh. Al-Ani, and M. F. Mosleh, "Outdoor millimeter-wave propagation simulation model for 5g band frequencies," in *2019 2nd International Conference on Electrical, Communication, Computer, Power and Control Engineering (ICECCPCE)*, 2019, pp. 40–45.

[13] G. R. Maccartney, T. S. Rappaport, S. Sun, and S. Deng, "Indoor office wideband millimeter-wave propagation measurements and channel models at 28 and 73 ghz for ultra-dense 5g wireless networks," *IEEE Access*, vol. 3, pp. 2388–2424, 2015.

[14] S.-F. Wang, B.-C. Lai, Y.-F. Hsu, and C.-A. Lu, "Dielectric properties of cao–b2o3–sio2 glass-ceramic systems in the millimeter-wave frequency range of 20–60 ghz," *Ceramics International*, vol. 47, no. 16, pp. 22 627–22 635, 2021. [Online]. Available: https://www.sciencedirect.com/science/article/pii/S0272884221013316

[15] S. Alekseev and M. Ziskin, "Reflection and absorption of millimeter waves by thin absorbing films," *Bioelectromagnetics*, vol. 21, no. 4, pp. 264–271.

[16] M. Jacob, T. Kürner, R. Geise, and R. Piesiewicz, "Reflection and transmission properties of building materials in d-band for modeling future mm-wave communication systems," in *Proceedings of the Fourth European Conference on Antennas and Propagation*, 2010, pp. 1–5.

[17] X. Liao, C. Lin, Y. Wang, and J. Zhang, "Measurements and characterization of reflection and transmission propagation of low-e glass for mmwave communications in smart buildings," in *2023 IEEE 11th Asia-Pacific Conference on Antennas and Propagation (APCAP)*, vol. volume1, 2023, pp. 1–2.

[18] M. Talib, N. Binti, N. Othman, and A. Sallomi, "The effect of urban environment on large-scale path loss model's main parameters for mmwave 5g mobile network in iraq," *Open Engineering*, 04 2024.

[19] M. I. Rochman, D. Fernandez, N. Nunez, V. Sathya, A. S. Ibrahim, M. Ghosh, and W. Payne, "Impact of device thermal performance on 5g mmwave communication systems," in *2022 IEEE International Workshop Technical Committee on Communications Quality and Reliability (CQR)*, 2022, pp. 1–6.

[20] V. Raghavan, A. Partyka, A. Sampath, S. Subramanian, O. H. Koymen, K. Ravid, J. Cezanne, K. Mukkavilli, and J. Li, "Millimeter-wave mimo prototype: Measurements and experimental results," *IEEE Communications Magazine*, vol. 56, no. 1, pp. 202–209, 2018.

[21] H. Kim, *Design and Optimization for 5G Wireless Communications*. Wiley, 2020, accessed: Sep. 23, 2024.

[22] L. Marabissi, Dania, R. Fantacci, and Spada, "A real case of implementation of the future 5g city," *Future Internet*, vol. 11, no. 1, 2019. [Online]. Available: https://www.mdpi.com/1999-5903/11/1/4

[23] A. Narayanan, M. I. Rochman, A. Hassan, B. S. Firmansyah, V. Sathya, M. Ghosh, F. Qian, and Z.-L. Zhang, "A comparative measurement study of commercial 5g mmwave deployments," in *IEEE INFOCOM 2022 - IEEE Conference on Computer Communications*, 2022, pp. 800–809.

[24] N. Foroughimehr, A. Wood, R. McKenzie, K. Karipidis, and A. Yavari, "Design and implementation of a specialised millimetre-wave exposure system for investigating the radiation effects of 5g and future technologies," *Sensors*, vol. 24, no. 5, 2024. [Online]. Available: https://www.mdpi.com/1424-8220/24/5/1516

[25] N. Foroughimehr, A. H. A. Clayton, and A. Yavari, "Exploring skin interactions with 5g millimeter-wave through fluorescence lifetime imaging microscopy," *Electronics*, vol. 13, no. 9, 2024. [Online]. Available: https://www.mdpi.com/2079-9292/13/9/1630